

This article was downloaded by: [Siauliu University Library]

On: 17 February 2013, At: 07:00

Publisher: Taylor & Francis

Informa Ltd Registered in England and Wales Registered Number: 1072954 Registered office: Mortimer House, 37-41 Mortimer Street, London W1T 3JH, UK



Advanced Composite Materials

Publication details, including instructions for authors and subscription information:

<http://www.tandfonline.com/loi/tacm20>

Size effect in particulate metal matrix composites: an analytical approach

Seung-Ho Kim & H. Thomas Hahn

Version of record first published: 02 Apr 2012.

To cite this article: Seung-Ho Kim & H. Thomas Hahn (2006): Size effect in particulate metal matrix composites: an analytical approach, *Advanced Composite Materials*, 15:2, 175-191

To link to this article: <http://dx.doi.org/10.1163/156855106777873888>

PLEASE SCROLL DOWN FOR ARTICLE

Full terms and conditions of use: <http://www.tandfonline.com/page/terms-and-conditions>

This article may be used for research, teaching, and private study purposes. Any substantial or systematic reproduction, redistribution, reselling, loan, sub-licensing, systematic supply, or distribution in any form to anyone is expressly forbidden.

The publisher does not give any warranty express or implied or make any representation that the contents will be complete or accurate or up to date. The accuracy of any instructions, formulae, and drug doses should be independently verified with primary sources. The publisher shall not be liable for any loss, actions, claims, proceedings, demand, or costs or damages whatsoever or howsoever caused arising directly or indirectly in connection with or arising out of the use of this material.

Size effect in particulate metal matrix composites: an analytical approach *

SEUNG-HO KIM ^{1,2,†} and H. THOMAS HAHN ^{1,3}

¹ *Mechanical and Aerospace Engineering Department, University of California, Los Angeles,
CA 90065, USA*

² *MTI Group, Samsung Corning Precision Glass Company Limited., ChungNam, Korea, 336-840*

³ *Materials Science and Engineering Department, University of California, Los Angeles,
CA 90065, USA*

Received 21 September 2004; accepted 11 July 2005

Abstract—This study briefly reviews various existing methods to account for the effect of particle size on the mechanical properties of particulate metal matrix composites. A simple and easy method is to use a size-dependent constitutive equation for the matrix. The suggested method does not require the development of a new computational algorithm and is compatible with any standard finite element software. Finite element analyses have been carried out to show how the deformation behavior of a metal matrix composite changes as the particle size and volume fraction are varied. The strain hardenings in metal matrix composites are increased with smaller particles and larger volume fractions which could not be predicted with size-independent constitutive relation. It has been shown that the suggested method can be used in a common finite element analysis process to account for the size effect of composite strengthening.

Keywords: Metal matrix composite; material length scale; particle size effect; finite element analysis.

1. INTRODUCTION

Metal matrix composites (MMCs) reinforced by particles, fibers or whiskers have been widely used in weight-saving applications such as automotive parts, space applications, defense systems, thermal composites as well as electronic substrates and packaging. Advantages of MMCs, which make them popular in various industries, are low density, high specific energy and high stiffness with good thermal properties and fatigue resistance. The improvements of mechanical properties in MMCs depend on the strength, the shape and the volume fraction of particles,

*Edited by the JSCM.

[†]To whom correspondence should be addressed. E-mail: seung-ho.kim@samsung.com

a particle–matrix interface, etc. Effects of the particle size on the mechanical properties have been observed in the micron range experimentally. The strength, yield stress and ductility of particulate MMC are known to increase with decreasing particle size [1–5]. Whether or not the same trend will continue into the nanometer range is not known experimentally. Therefore, it is worthwhile to investigate analytically how much strengthening can be achieved by using nanoparticles.

A number of analytical approaches have been proposed to predict the observed particle size effect in MMCs. They include the discrete dislocation theory [6, 7], the non-local plasticity [8, 9], the strain gradient method [10, 11], and the size-dependent constitutive equation method [12, 13]. Of these different methods, only the size-dependent constitutive equation method allows the use of readily available finite element software with modified constitutive relations. The other methods require new computational algorithms, and are difficult to use readily.

This study briefly reviews various methods to account for the size effect in metal matrix composites. The method based on the use of a size-dependent constitutive equation has been chosen for further study. When used in the ABAQUS/Standard commercial code, the method is shown to be able to predict the effect of particle size and the particle volume fraction in SiC/aluminum composites.

2. SIZE-INDEPENDENT PLASTICITY

Finite element analyses with classic size-independent (SI) plasticity are carried out for the material characterization of Al–Al₂O₃ composites with respect to the particle size and volume fractions. ABAQUS/Standard, commercial implicit elastic–plastic finite element code, is employed for numerical simulations. Linear quadrilateral plane strain elements (CPS4) are adopted. 740 nodes and 720 elements are used for the composite with one reinforcement. Matrix material is modeled by piecewise linear hardening plasticity and reinforcement by linear elastic material. Geometric and material nonlinearities are considered with large deformation formulations. Figure 1 shows material properties and boundary conditions with initial mesh system for the simulation. Symmetric boundary conditions are imposed on the symmetric line at $x = 0$ and $y = 0$, respectively. Periodic boundary conditions are imposed on the upper side as shown in the Fig. 1b. Uniform axial extension of 2% strain is imposed by displacement boundary conditions at the right end. Analyses are carried out with respect to the particle diameter varied from 40 nm to 320 nm at the particle volume fraction of 20%. Figure 2 shows initial mesh systems with the number of nodes and elements for the analysis with respect to the particle size. The number of reinforcements is increased with smaller particles since identical representative volumes of MMC are used to inspect the particle size effect. Figure 3a and b shows distributions of calculated von Mises stress and plastic strain, respectively, with respect to the particle size. High stresses are developed in reinforcements and plastic deformations are concentrated on the matrix near border of reinforcements. Figure 4 explains the comparison of true stress–strain curves

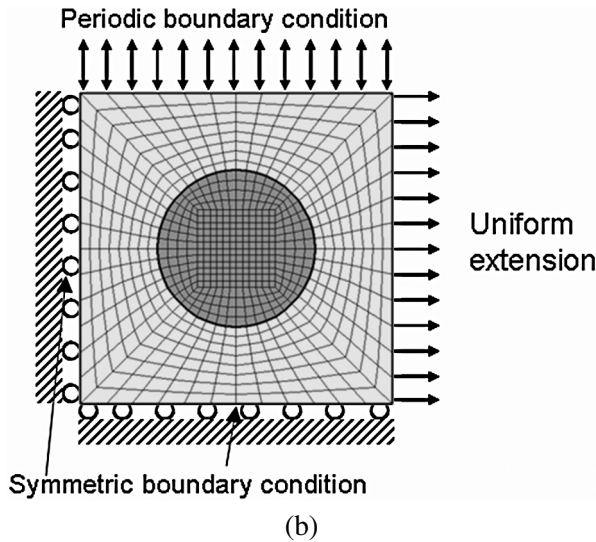
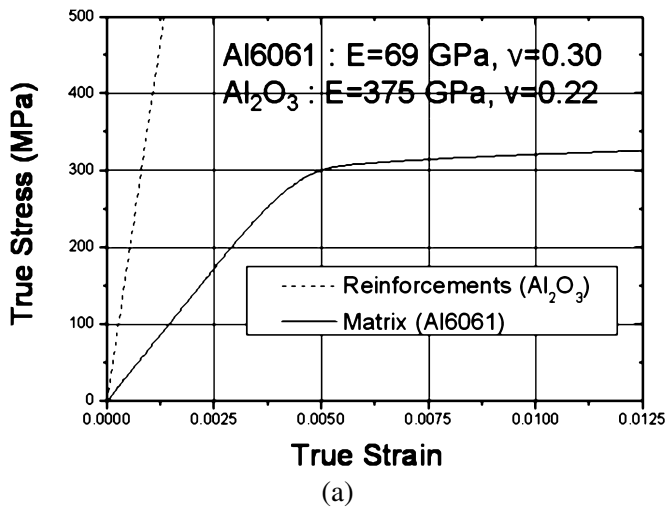
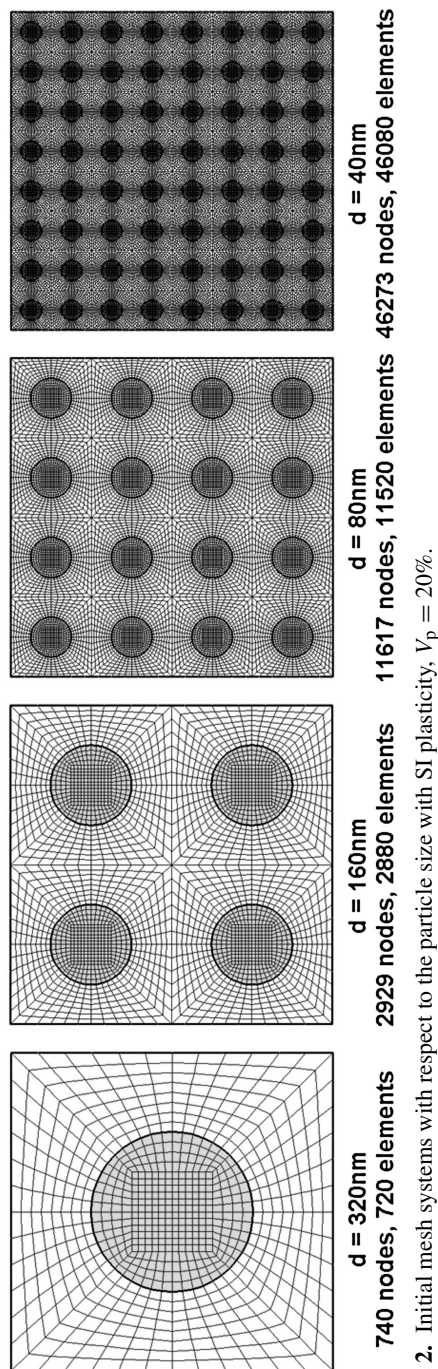


Figure 1. Material properties and boundary conditions with initial mesh system for the simulation with SI plasticity.

calculated from analyses with respect to the particle size. Distributions of process variable can be calculated to estimate material behaviors of MMC. However, the effect of the particle size in MMC could not be explained by SI plasticity, since it does not contain material length scale or gradient effect to reflect interactions among particles and dislocations. Figure 5 explains the comparison of true stress–strain curves with respect to the particle volume fraction. Moduli and yield stresses are increased with larger volume fraction of particles. However, there are relatively small work hardening effects even with high volume fraction of particles. Analysis



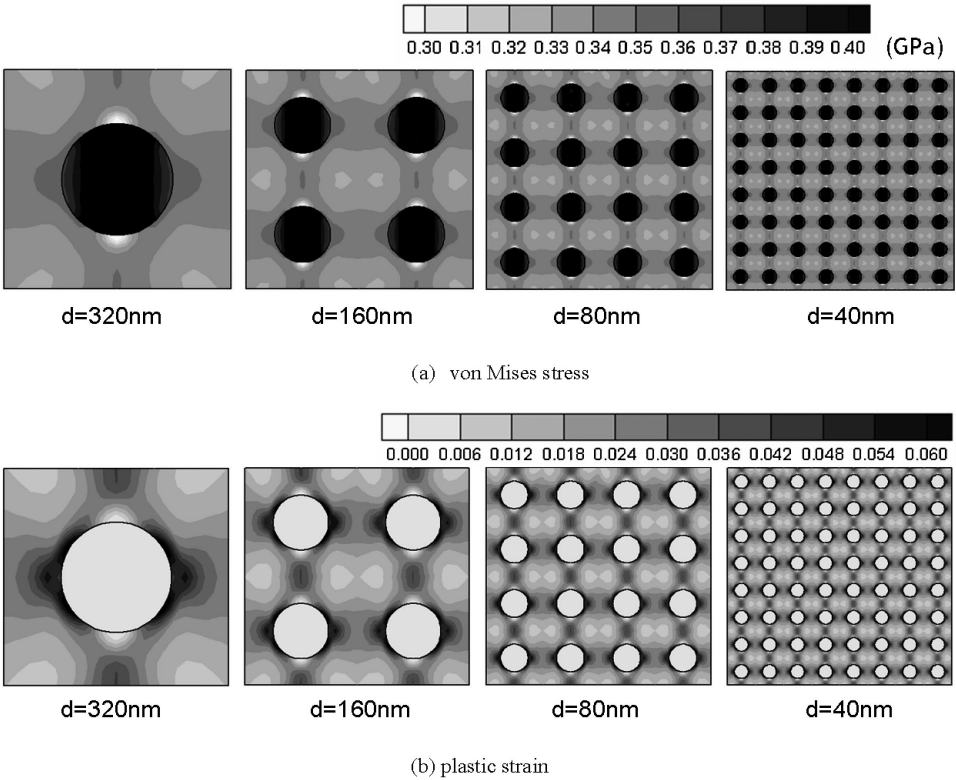


Figure 3. Distributions of calculated variables with respect to the particle size from SI plasticity; applied strain = 0.02, $V_p = 20\%$. (a) von Mises stress, (b) plastic strain.

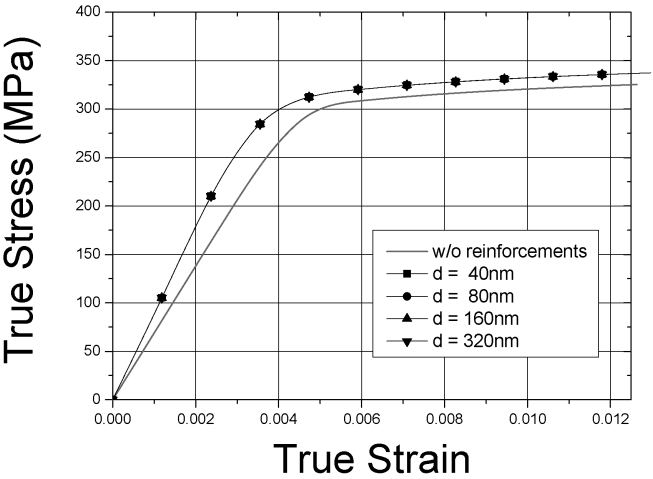


Figure 4. Comparison of true stress–strain curves with respect to the particle size from SI plasticity, $V_p = 20\%$.

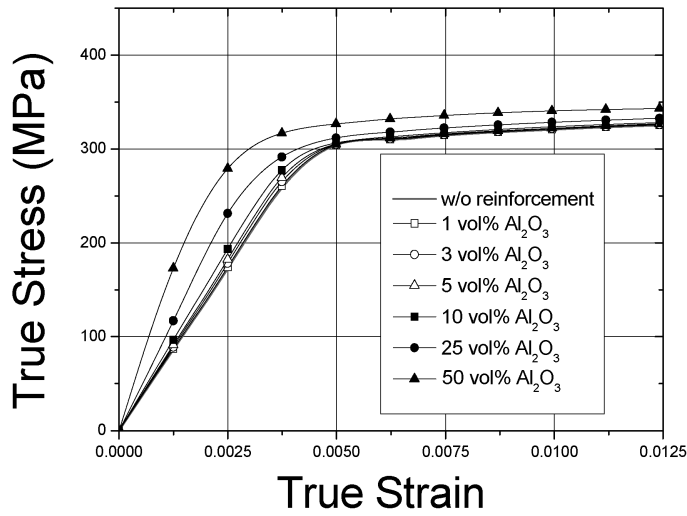


Figure 5. Comparison of true stress–strain curves with respect to the particle volume fraction from SI plasticity.

results show that the classical SI plasticity cannot account for the effects of particle size and volume fraction on strain hardening.

3. ANALYTICAL APPROACHES TO THE SIZE EFFECT

SI plasticity based on continuum mechanics has difficulties in predicting mechanical properties effectively with different particle size and volume fraction of reinforcements in MMC. A localized dislocation model or molecular dynamics could be employed with fine particle size, but it is still difficult to apply to various realistic analysis models due to complicated formulations and prolonged computation times. A number of analytical approaches are suggested to explain the size effect of particles in MMC. They include the discrete dislocation theory, the non-local plasticity, the strain gradient method, and the size-dependent constitutive equation method. This study briefly reviews those methods to account for the size effect in MMC.

3.1. Dislocation plasticity

In a dislocation plasticity [6, 7], dislocations are modeled by linear defects and can be generated or annihilated during the deformation of composites, from which mechanical characteristics of metal matrix can be modified in consideration of dislocation model. The current state of the body in terms of displacement, strain and stress fields can be written as the superposition of two fields,

$$u_i = \tilde{u}_i + \hat{u}_i, \varepsilon_{ij} = \tilde{\varepsilon}_{ij} + \hat{\varepsilon}_{ij}, \sigma_{ij} = \tilde{\sigma}_{ij} + \hat{\sigma}_{ij}. \quad (1)$$

The ($\tilde{}$) fields are associated with the dislocations in their current configuration but in an infinitely large medium of the homogeneous matrix material. There

fields can be obtained by superposition of the fields associated with each individual dislocation.

$$\tilde{u}_i = \sum_{\kappa} \tilde{u}_i^{\kappa}, \tilde{\varepsilon}_{ij} = \sum_{\kappa} \tilde{\varepsilon}_{ij}^{\kappa}, \tilde{\sigma}_{ij} = \sum_{\kappa} \tilde{\sigma}_{ij}^{\kappa}. \quad (2)$$

Dislocations can be moved, created or annihilated during the analysis. In each analysis step, there are three main computational stages: (i) determining Peach-Koehler forces acting on the dislocations; (ii) determining the rate of change of dislocation structures, which is related to the motion of dislocations; (iii) determining the stress and strain state for the current dislocation arrangement. The Peach-Koehler force on the k -th dislocation can be expressed as equation (3).

$$f^{\kappa} = \sigma_{12}^{\kappa} b. \quad (3)$$

Physically, the size effect is the result of dislocation motion being impeded by the particles. This effect will naturally depend on the distance between particles, which varies with the particle size at the same particle volume fraction.

3.2. Nonlocal plasticity

Another approach, called the non-local plasticity [8, 9], is to use the classical plasticity theory with the instant tangent modulus E_t replaced by,

$$E_t = \frac{E}{n} \left(\frac{\varepsilon_e^p}{\varepsilon_o} + 1 \right)^{1/n-1} \left[1 + \frac{l^2 \alpha^2}{(\varepsilon_o + \kappa \varepsilon_e^p)^2} \right]^{1/2}, \quad (4)$$

where E is the Young's modulus, n is the strain hardening exponent, ε_o is the yield strain, and ε_e^p is the effective plastic strain. With the proper selection of the material length l and the coefficient κ , the size effect is accounted for by the maximum plastic strain gradient α .

3.3. Strain gradient plasticity

In a composite, the strain gradient in the matrix depends on the size of the reinforcement phase at the same volume fraction. One of the approaches to account for the size effect is thus to use the strain gradient theory of plasticity for the matrix [10, 11]. In this approach, the strain tensor and strain gradient tensor can be expressed as equation (5).

$$\varepsilon_{ij} = \frac{1}{2}(u_{i,j} + u_{j,i}), \quad \eta_{ijk} = u_{k,ij}. \quad (5)$$

The equilibrium equation can be expressed by equation (6) including differential term of higher-order stress.

$$\sigma_{ik,i} - \tau_{ijk,ij} = 0. \quad (6)$$

Higher-order stresses τ_{ijk} are included in the equilibrium equations and stress–strain relations are taken as:

$$\sigma = \sigma_{ref} \sqrt{f^2(\varepsilon) + l\eta}, \quad f(\varepsilon) = \varepsilon^n, \quad \varepsilon = \sqrt{\frac{2}{3} \varepsilon'_{ij} \varepsilon'_{ij}}, \quad \eta = \frac{1}{2} \sqrt{\eta'_{ijk} \eta'_{ijk}}, \quad (7)$$

$$\sigma_{ij} = K \varepsilon_{kk} \delta_{ij} + \frac{2}{3} \frac{\sigma}{\varepsilon} \varepsilon'_{ij}, \quad l = 18\alpha^2 \left(\frac{\mu}{\sigma_{ref}} \right)^2 b, \quad (8)$$

$$\tau_{ijk} = l_\varepsilon^2 \left[\frac{1}{6} K \eta_{ijk}^H + \frac{\sigma}{\varepsilon} (\Lambda_{ijk} - \Pi_{ijk}) + \frac{\sigma_{ref}^2 f(\varepsilon) f'(\varepsilon)}{\sigma} \Pi_{ijk} \right].$$

Here σ_{ref} is the reference stress in uniaxial tension, ε_{ij} is the strain tensor, η_{ijk} is the strain gradient tensor, K is the bulk modulus, Λ_{ijk} is a function of η_{ijk} , and Π_{ijk} is a function of ε_{ij} and η_{ijk} . The material lengths l and l_ε are both related to the Burgers vector.

3.4. Size-dependent (SD) plasticity

Although all the aforementioned approaches can be used to explain the increase of strain hardening in MMC with decreasing particle size, their implementation is not straightforward as they require new computational schemes which are not readily available in commercial finite element software. Nevertheless, it should be pointed out that the material lengths used in these approaches do not require *a priori* knowledge of the particle size, and hence the effect of particle size is predicted *a posteriori*.

An alternative approach based on the classical plasticity theory has been proposed by Nan and Clarke [12]. In this approach, the formalism of classical plasticity is still maintained:

$$\varepsilon = \frac{\sigma}{E} + c \frac{\sigma_o^m}{E} \left(\frac{\sigma}{\sigma_o^m} \right)^{1/n}, \quad (9)$$

where σ_o^m is the yield strength and c is a dimensionless constant. However, σ_o^m is no longer constant but replaced by σ_o^m which changes with effective plastic strain:

$$\sigma_o^m = \sigma_o + \Delta\sigma^m, \quad (10)$$

$$\Delta\sigma^m = \sigma_{or} + \sigma_{iso} + \sigma_{kin} = \alpha\mu b \sqrt{\frac{4V_p}{\pi d^2}} + \beta\mu \sqrt{\frac{b\varepsilon_e^p V_p}{d}} + \gamma\mu V_p \sqrt{\frac{b\varepsilon_e^p}{d}}. \quad (11)$$

The first term in equation (11) is the Orowan stress, the stress required to pass a dislocation through an array of impeding particles of diameter d . The second and third terms are related to isotropic and kinematical strain gradient effects, respectively, associated with geometrically necessary dislocations [12]. In the equation, V_p is the particulate volume fraction, μ is the shear modulus, b is the Burgers vector, and $\alpha(\sim 1)$, $\beta(\sim 0.4)$, and $\gamma(\sim 2)$ are constants.

As is clear, the use of the size-dependent constitutive equation requires *a priori* knowledge of the particle size, i.e. the constitutive equation should be modified depending on the particle size. Nevertheless, it is readily amenable to implementation in a commercial finite element software. Therefore, this approach, represented by equations (9–11), was chosen to study the stress–strain behavior of SiC/aluminum composites.

4. FINITE ELEMENT ANALYSERS WITH SIZE-DEPENDENT PLASTICITY

Finite element analyses were carried out using ABAQUS/Standard on SiC/aluminum composites using the size-dependent constitutive equations. Both two- and three-dimensional analyses were performed to make a quantitative comparison of state variables. A square with one particle at its center was chosen as the representative volume element for two-dimensional analysis, and a cube with one particle at its center for three-dimensional case. One-fourth of the square and one-eighth of the cube were used, respectively, in view of the symmetry. A uniform displacement was applied on the right-side boundary in the x-direction and all the boundaries were kept flat. In order to simulate a uniaxial stress condition, the side boundaries were allowed to move to satisfy the effective traction-free boundary condition. The material properties used are listed in Table 1 [12]. Figure 6a and b shows initial representative mesh systems for two- and three-dimensional analyses, respectively. A total of 420 linear quadrilateral elements were used for two-dimensional analysis and 1728 linear brick elements for three-dimensional analysis. Figure 7 shows distributions of von Mises stress calculated from SI plasticity and SD plasticity. Higher stresses are developed in the results from SD plasticity since strain hardening of matrix was pre-assumed by constitutive equations in consideration of the particle size effect, volume fractions and dislocation motions. Figure 8 explains development of yielding regions with respect to axial deformations for two-dimensional analysis. Matrix yielding began on the axial region near the reinforcement border and became wider, while another yielding occurs on the top-central region. Figure 9 compares predicted stress–strain relations for composites. Three-dimensional analyses are seen to agree better with experimental data [1] than two-dimensional results for two different particle sizes. As expected, the size-dependent constitutive equation with $d = 7.5 \mu\text{m}$ gives higher stresses than the standard constitutive equation. It should be noted that the standard constitutive equation does not yield any size effect on the composite stress–strain relation. Figure 10 compares plastic dissipation energy

Table 1.
Material properties

Material	E (GPa)	μ (GPa)	σ_o (MPa)	n	c
Aluminum matrix (Al 356 T4)	70.0	26.3	86	0.212	0.429
SiC particle	427	182	N/A	N/A	

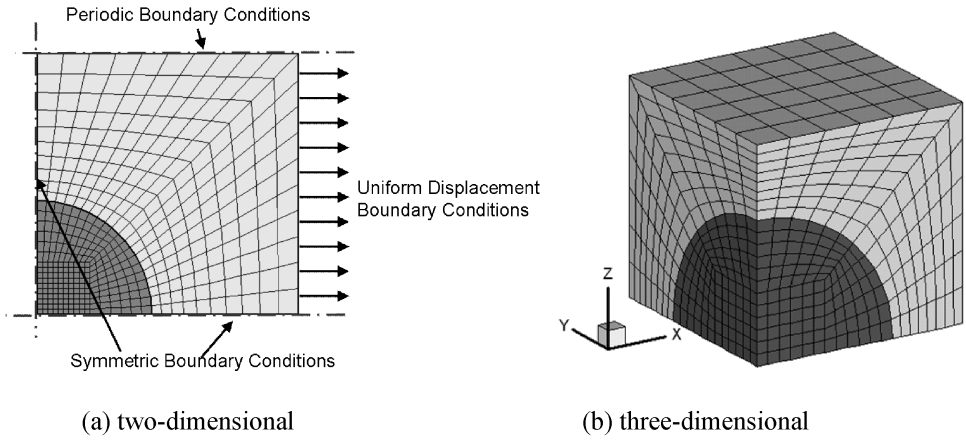


Figure 6. Initial representative mesh system for the analyses with SD plasticity. (a) two-dimensional, (b) three-dimensional.

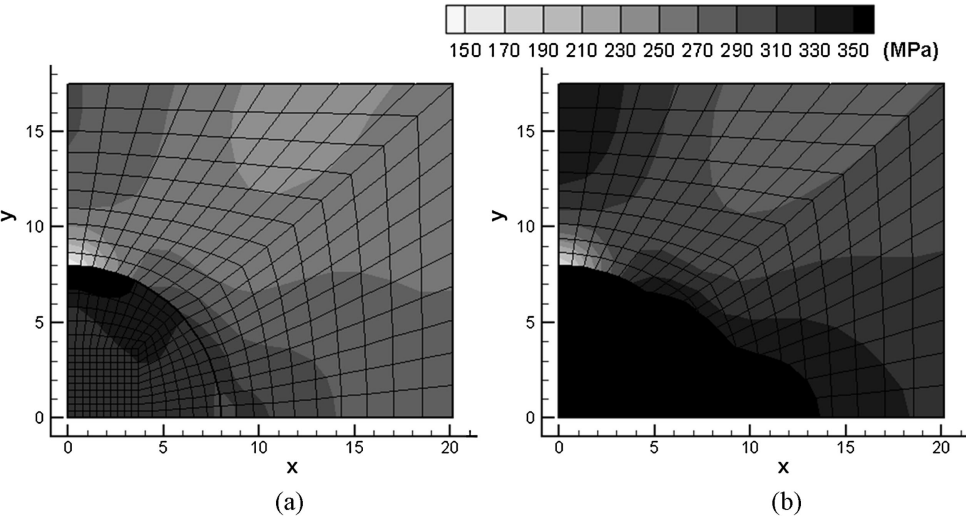


Figure 7. Comparison of von Mises stress distributions from two-dimensional analysis, applied strain = 0.05, particle diameter = 16 μm , $V_p = 15\%$. (a) SI plasticity, (b) SD plasticity.

densities per unit volume (μm^3) for both two- and three-dimensional cases. Larger plastic dissipations occurred in three-dimensional results since a particle diameter is larger for the three-dimensional case at the identical volume fraction of particles, which induced higher strain hardening of the matrix from equation (11). As a matter of course, SD plasticity results predicted higher plastic deformation than SI plasticity on account of strengthening that originated from the particle size effect.

The particle sizes were varied to 0.01 μm to 50 μm in order to observe the particle size effect up to the nano-scale and to compare SD plasticity results with other analytical approaches. Stress-strain relations of the matrix are modified with

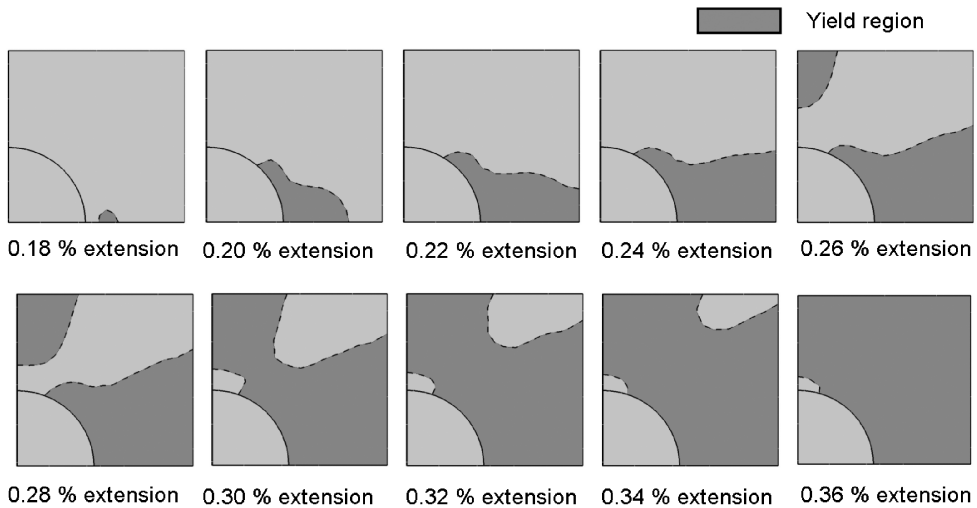


Figure 8. Development of yielding region in the matrix from the two-dimensional analysis.

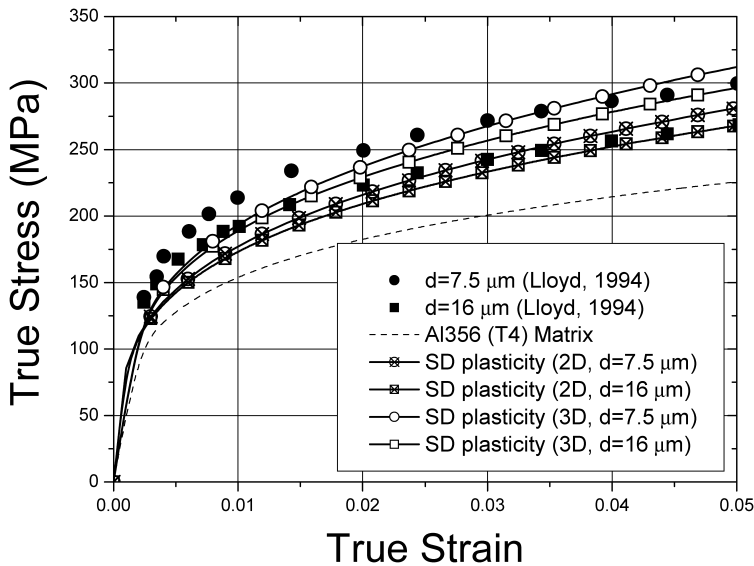


Figure 9. Predicted size effects compared with experimental data: $V_p = 15\%$.

SD constitutive equations as compared in Fig. 11. Strain hardenings exponentially increase with the decrease of the particle size, which looks like exaggerating in nano-scale range in some measure. The SD constitutive equations are known to show good agreements in micron scale; however, strengthening effects in nano-scale need to be explored and verified with experimental results. Figure 12 compares von Mises stress distributions from three-dimensional results with respect to the particle size for a particle volume fraction of 15%. As expected, the von Mises stresses are higher when the particles are smaller.

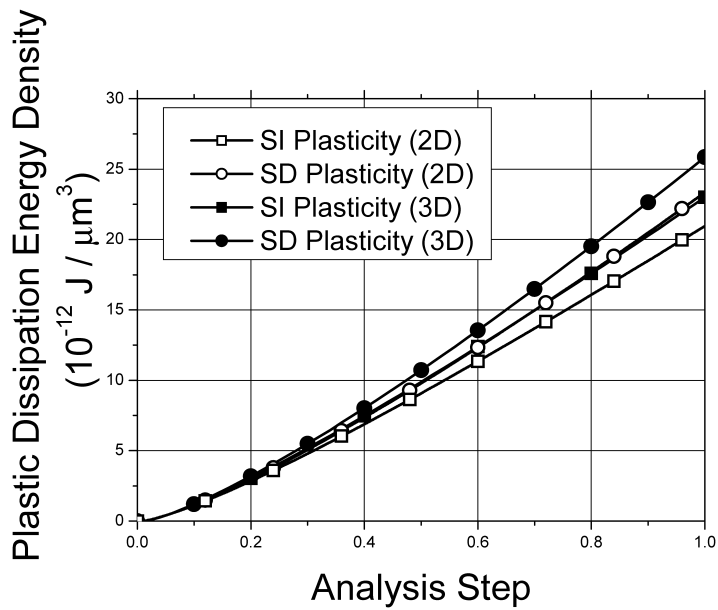


Figure 10. Comparison of plastic dissipation energy densities: $V_p = 15\%$.

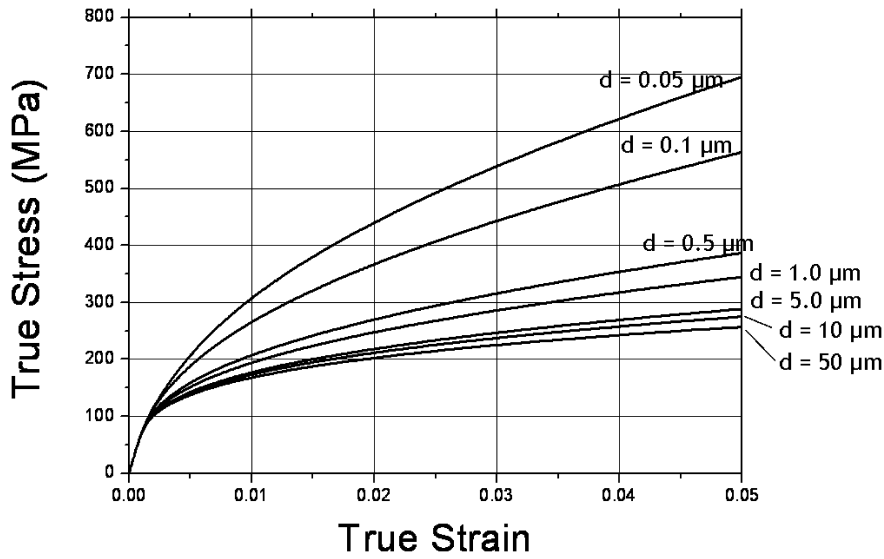


Figure 11. Comparison of elastic-plastic stress-strain curves of matrix for SD plasticity with respect to the particle size.

The method of size-dependent constitutive equation is compared with the strain gradient method [11] in Fig. 13. Both methods are seen to yield almost the same composite stress-strain relations, regardless of the particle size. Further, Fig. 14 indicates that the effective medium method [12], not a detailed finite

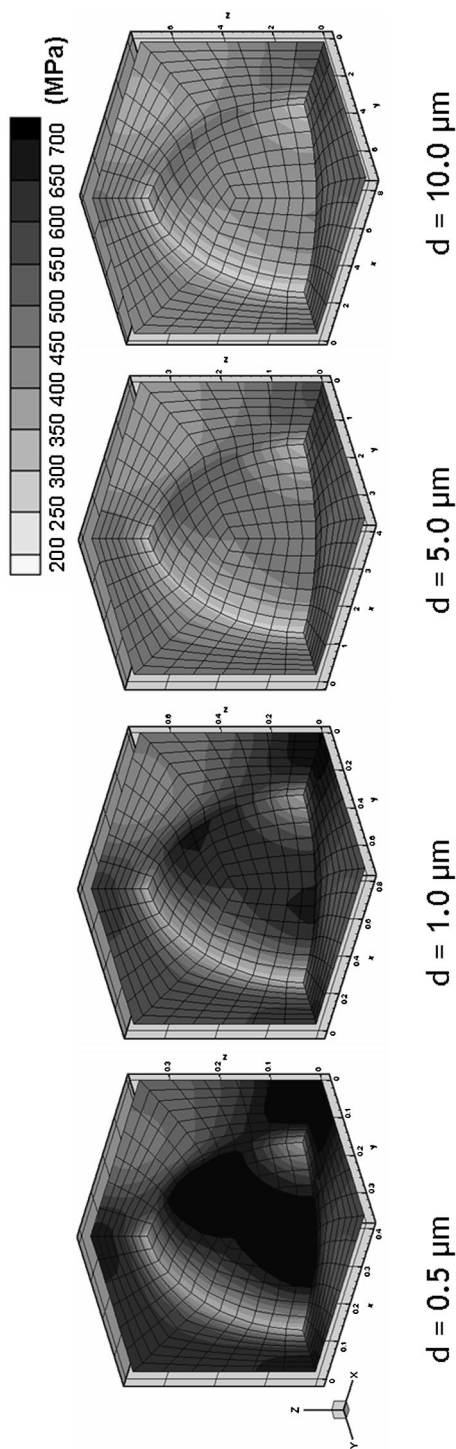


Figure 12. Von Mises stresses decreasing with increasing particle size: $V_p = 15\%$, applied strain = 0.05.

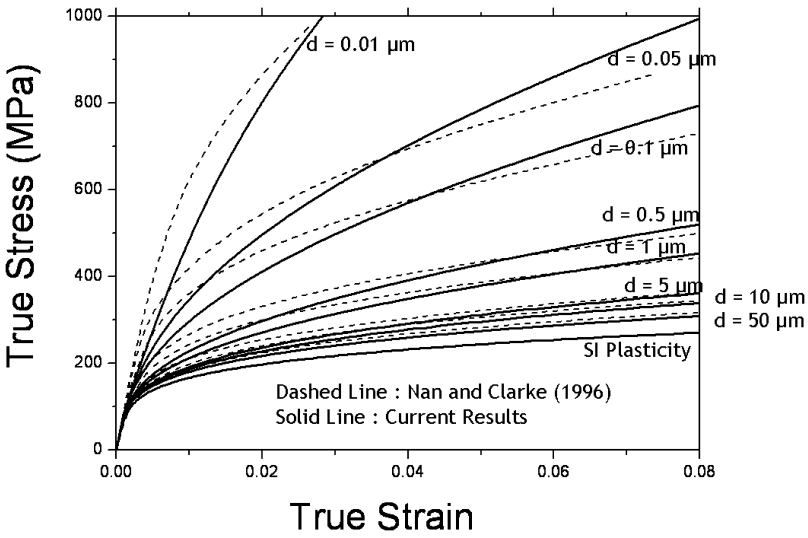


Figure 13. Composite stress–strain relations predicted by finite element analysis using SD constitutive equation, $V_p = 15\%$: comparison with the effective medium method.

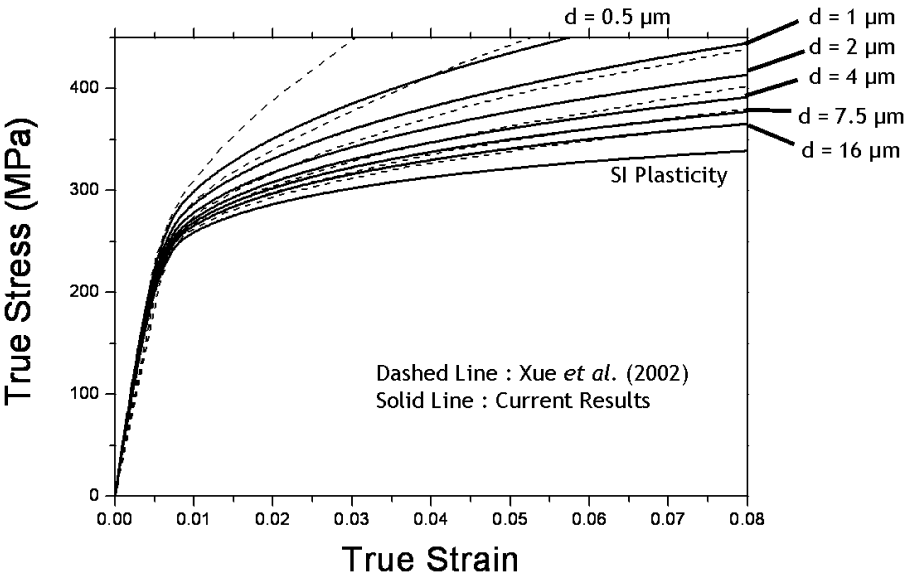


Figure 14. Composite stress–strain relations predicted by finite element analysis using SD constitutive equation, $V_p = 15\%$: comparison with the strain gradient method.

element method, can be used for the prediction of composite stress–strain relations. Figure 15a and b, shows effects of particle volume fraction on the von Mises stresses and plastic distributions, respectively. Von Mises stresses and plastic deformations are increasing with increasing particle volume fraction. Figure 16 compares true stress–strain relations with respect to the particle volume fraction. Higher strain

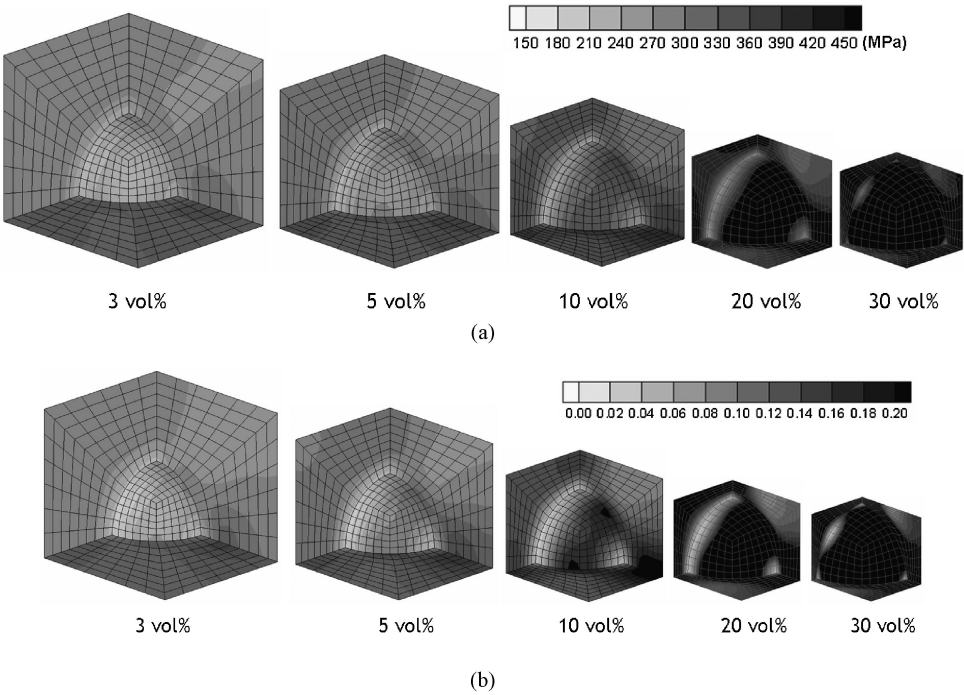


Figure 15. Effect of particle volume fraction: particle diameter = $7.5\ \mu\text{m}$; applied strain = 0.05. (a) on von Mises stress distributions, (b) on plastic strain.

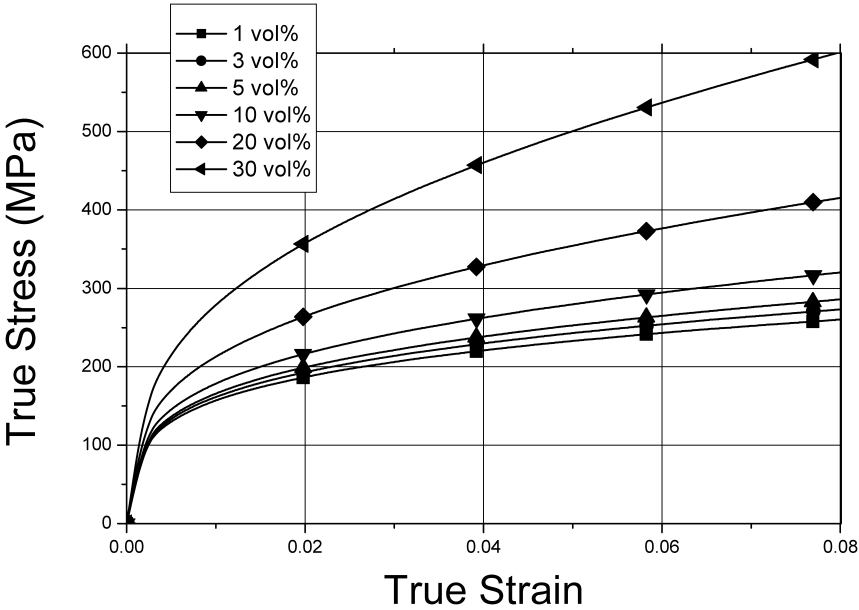


Figure 16. Effect of particle volume fraction on composite stress–strain relations.

hardening occurred with SD plasticity, which could not be predicted from SI plasticity. For example, the theory predicts that at 4% strain, the composite can carry more than double the stress that the aluminum matrix can carry when 50-nm SiC particles are added. However, one drawback would be poor ductility resulting from large plastic strains in the matrix. Such projections still remain to be verified by experiments.

5. CONCLUSIONS

The increased strain hardening observed in metal matrix composites with smaller particles is the result of the increasing difficulty of dislocation motion associated with smaller inter-particle spacing. Such strengthening effect can be explained by a number of theories. Unfortunately, those theories that can explain the size effect without a prior knowledge of the particle size call for the development of new computational algorithms. However, it has been shown that a size-dependent constitutive relation can be used in standard finite element software to account for the size effect of composite strengthening.

Acknowledgement

This study is based on work supported by the Office of Naval Research through Grant N00014-02-1-0642(1) (HTH) with Dr. Y. Rajapakse as the Program Officer and by the Korea Science and Engineering Foundation (KOSEF) through Overseas Post-doctoral Fellowships Grant M01-2003-000-10014-0 (SHK).

REFERENCES

1. D. J. Lloyd, Particle reinforced aluminum and magnesium matrix composites, *Int. Mater. Rev.* **39**, 1–23 (1994).
2. N. Chawla and Y. L. Shen, Mechanical behavior of particle reinforced metal matrix composites, *Adv. Eng. Mater.* **3**, 357–370 (2001).
3. O. Sbaizero and G. Pezzotti, Influence of the metal particle size on toughness of Al₂O₃/Mo composite, *Acta Mater.* **48**, 985–992 (2000).
4. M. Kouzeli and A. Mortenson, Size dependent strengthening in particle reinforced aluminium, *Acta Mater.* **50**, 39–51 (2002).
5. Y. L. Shen, J. J. Williams, G. Piotrowski, N. Chawla and Y. L. Guo, Correlation between tensile and indentation behavior of particle-reinforced metal matrix composites: An experimental and numerical study, *Acta Mater.* **49**, 3219–3229 (2001).
6. E. V. D. Giessen and A. Needleman, Discrete dislocation plasticity: a simple planar model, *Modelling Simul. Mater. Sci. Eng.* **3**, 689–735 (1995).
7. H. H. M. Cleveringa, E. V. D. Giessen and A. Needleman, Comparison of discrete dislocation and continuum plasticity predictions for a composite material, *Acta Mater.* **45**, 3163–3179 (1997).
8. C. F. Niordson and V. Tvergaard, Nonlocal plasticity effects on the tensile properties of a metal matrix composite, *Eur. J. Mech. A/Solids* **20**, 601–613 (2001).
9. A. Acharya and J. L. Bassani, Lattice incompatibility and a gradient theory of a crystal plasticity, *J. Mech. Phys. Solids* **48**, 1565–1595 (2000).

10. N. A. Fleck and J. W. Hutchinson, A phenomenological theory for strain gradient effects in plasticity, *J. Mech. Phys. Solids* **41**, 1825–1857 (1993).
11. Z. Xue, Y. Huang and M. Li, Particle size effect in metallic materials: a study by the theory of mechanism-based strain gradient plasticity, *Acta Mater.* **50**, 149–160 (2003).
12. C. W. Nan and D. R. Clarke, The influence of particle size and particle fracture on the elastic/plastic deformation of metal matrix composites, *Acta Mater.* **44**, 3801–3811 (1996).
13. C. W. Nan and D. R. Clarke, Modeling the elastic-plastic deformation of Al/Al₂O₃ particulate composites, *J. Am. Ceram. Soc.* **80**, 237–240 (1997).